Office of Naval Research

Contract N00014-J-1276

Technical Report No. UWA/DME/TR-93/73

STEEP GEOMETRIC GRATING FOR USE IN MOIRÉ INTERFEROMETRY

by

F.X. Wang, G.B. May and A.S. Kobayashi

July 1993

The research reported in this technical report was made possible through support extended to the Department of Mechanical Engineering, University of Washington, by the Office of Naval Research under Contract N00014-89-J-11276. Reproduction in whole or in part is permitted for any purpose of the United States Government.

Department of Mechanical Engineering

College of Engineering

University of Washington

STEEP GEOMETRIC GRATING FOR USE IN MOIRÉ INTERFEROMETRY

F.X. Wang, G.B. May and A.S. Kobayashi

University of Washington

Department of Mechanical Engineering

Seattle, Washington 98195, USA

Abstract

The theoretical background and the procedure of executing a new moiré interferometry method, which combines the advantages of geometric moiré method with the traditional moiré interferometry, is reported. The method uses a steep geometric grating of about 40 lines/mm on a mirror finished specimen surface to achieve high contrast moiré fringes. A special four beam moiré interferometry bench is designed for the low grating frequency used. An application to experimental fracture mechanics analysis is briefly discussed.

Introduction

Conventional geometric moiré (grating spatial frequency $f \leq 40$ lines/mm) utilizes a specimen grating, which is projected on to a reference grating on the camera screen and generates a geometric interference pattern. The major advantage of this method is its capacity for measuring large deformation. The main disadvantage is its poor contrast, especially when the specimen grating is generated by reflection from opaque materials.

Moiré interferometry (grating spatial frequency: $f \approx 2000$ lines/mm) utilizes the interference between two diffracted beams of a coherent light. Its advantages include high sensitivity and good contrast. One of its disadvantages is that the specimen grating is destroyed with large

deformation, especially in the plastically deformed region where the moiré pattern is lost and a uniformly dark pattern is observed. Moreover, under large deformation, the surface of the specimen is warped, and the diffracted beam is projected away from the object lens and the camera making it difficult to photograph the warped moiré patterns.

In this paper, we report on a new moiré interferometry which uses a steep geometric grating. The method combines the advantages of the geometric and the traditional moiré interferometry methods and eliminates the two disadvantages mention above.

Theory

The essence of moiré interferometry can be considered as a special application of strain analysis using holography. Holography normally consists of two main operations, i.e. information recording and reconstruction.

First, a sinusoidal wave grating is generated by exposing the two coherent, interfered oblique collimated beams, i.e. object beam and reference beam, on the emulsion side of a holographic plate. After being linearly developed and fixed, the contrast of the hologram shows the amplitudes of the two beams. The spatial structure, i.e. the profile and the pitch between these parallel inference of the sinusoidal waves record the phase angles of the two wave fronts.

Second, the moiré interferometry is a process of reconstructing the wave fronts of the object beams. Moiré interferometry adopts two beams with a specific and symmetric entrance angle to illuminate the specimen. The superposition of the plus and minus first order object beams of the deformed grating generates the wave front interference fringes. These fringes carry the information of the specimen deformation.

From the Hugens-Fresnel theory, the wave fronts of the secondary waves interfere and determine the distribution of the light field. The mathematical model is the Fresnel-Kirchhoff diffraction formula or the "the unique boundary solution for the infinite sourceless space." Briefly speaking, when there is a change on the boundary, the light field will be redistributed, and the solution is unique. Therefore, the wave front reconstruction is also unique and can be observed only from a specific direction.

Rectangular grating also can be considered as a hologram, however, it is generated by illuminating a series of collimated lights interfering with the 0 order reference light at different entrance angles ($\sin\theta_1=\pm m\lambda f\leq 1$) with different intensities. These lights interfere and superimpose at the film plane and create a hologram. Therefore, when a pair of beams illuminate symmetrically a specimen, corresponding reconstructions of the interference between 0, ±1, , ±2, ..., ±m, order diffraction object beams overlay as shown in Fig. 2.(d) results. The interference pattern is unique, but, there are $(2m)^2$ orders for the different diffraction directions. When these diffraction beams, which carry the same black and white fringe pattern shine on the screen of the grating surface, the dark areas become black lines and the bright areas appear as white lines. Therefore, the interference pattern can be observed on the specimen surface from any direction.

A black and white cross grating illustrated as an orthogonal matrix is shown in Fig.1. The matrix consists of two arraying quasi-periodic unit rectangular functions along the x and y axes. Assuming x,y symmetry, both arrays are composed of a finite odd number, N, of terms. The Grit-Functions, G(x) and G(y), are defined as follows

$$G(x) = \sum_{n=\frac{-(N-1)}{2}}^{\frac{N-1}{2}} \text{Rect}[x + nd]$$

$$G(y) = \sum_{n=\frac{-(N-1)}{2}}^{\frac{N-1}{2}} \text{Rect}[y + nd]$$

where d is the spatial period of the grating and the unit rectangular functions, Rect[x] and Rect[y], are

$$\text{Rect}[x] = \begin{cases} H & \text{when } |x| < d/2 \\ 0 & \text{when } |x| > d/2 \end{cases}$$

$$\text{Rect}[y] = \begin{cases} H & \text{when } |y| < d/2 \\ 0 & \text{when } |y| > d/2 \end{cases}$$

The transparent rate function, T(x,y), or the reflective rate function, R(x,y), of the grating is the product of a Grit-functions G(x) and G(y). or

$$T(x,y) = R(x,y) = G(x) \cdot G(y)$$

Consider a coherent laser beam, A, with a plane wave-front, which is projected normally on to the grating, as shown in Fig. 2(a). The normal Fraunhoffer diffraction field, $U_n[x',y']$, can be calculated by the Fourier transformation on the spectral plane which is composed of a two dimensional orthogonal array of diffraction points.

$$\begin{aligned} U[X',Y']_n &= \mathcal{F}\{A \cdot [T(X,Y)]\} \\ &= \mathcal{F}\{A \cdot G(x) \cdot G(y)] \\ &= A \cdot \mathcal{F}[G(X)] \cdot \mathcal{F}[G(Y)] \\ &= A \cdot \frac{\text{Sin}(\pi d \cdot fx/2)}{\pi d \cdot fx/2} \cdot \frac{\text{Sin}(N\pi d \cdot fx)}{\text{Sin}(\pi d \cdot fx)} \cdot \frac{\text{Sin}(\pi d \cdot fy/2)}{\pi d \cdot fy/2} \cdot \frac{\text{Sin}(N\pi d \cdot fy)}{\text{Sin}(\pi d \cdot fy)} \end{aligned}$$

$$= A \cdot \mathrm{Sinc}(d \cdot f_x/2) \cdot \frac{\mathrm{Sin}(N\pi d \cdot fx)}{\mathrm{Sin}(\pi d \cdot fx)} \cdot \mathrm{Sinc}(d \cdot f_y/2) \cdot \frac{\mathrm{Sin}(N\pi d \cdot fy)}{\mathrm{Sin}(\pi d \cdot fy)}$$

where symbol "$\mathcal{F}$" represents the Fourier transformation and the terms, $\mathrm{Sinc}(d \cdot f_x/2)$ and $\mathrm{Sinc}(d \cdot f_y/2)$, represent the diffraction factors of the unit rectangular functions, Rect[x] and Rect[y], in the x and y directions of the grating, respectively. The product of the two terms comprises a two-dimensional amplitude envelop surface.

Furthermore, the terms $\frac{\mathrm{Sin}(N\pi d \cdot f_x)}{\mathrm{Sin}(\pi d \cdot f_x)}$ and $\frac{\mathrm{Sin}(N\pi d \cdot f_y)}{\mathrm{Sin}(\pi d \cdot f_y)}$ represent the interference factors between the rectangular functions of N units. f_x and f_y are the independent variable frequencies of the grating along the x and y axes. Let λ represent the wave-length of the incident light and F be the focal length of the Fourier transform lens. With the grating in front of the focal plane of the lens, the condition of an iso-optical path must be satisfied or for the x' - y' spectrum plane

$$f_x = \frac{x'}{\lambda F} \; ; \; f_y = \frac{y'}{\lambda F} \quad \text{or} \quad x' = \lambda F f_x \; ; \; y' = \lambda F f_y$$

If $d \cdot f_x = i$ and $d \cdot f_y = j$, where i and j are arbitrary integer number, then, $\mathrm{Sin}(N\pi d \cdot f_x) = 0$; $\mathrm{Sin}(\pi d \cdot f_x) = 0$, and $\mathrm{Sin}(N\pi d \cdot f_y) = 0$; $\mathrm{Sin}(\pi d \cdot f_y) = 0$.

Since the ratio $\frac{\mathrm{Sin}(N\pi d \cdot f_x)}{\mathrm{Sin}(\pi d \cdot f_x)} = \frac{\mathrm{Sin}(N\pi d \cdot f_y)}{\mathrm{Sin}(\pi d \cdot f_y)} = N$

many principal maximums are created by the interference factor of N unit rectangular function which consists of the diffraction points, i.e. a 2i x 2j matrix in the spectrum plane. These points form an array at the positions $x' = i \cdot \frac{\lambda F}{d}$; $y' = j \cdot \frac{\lambda F}{d}$. The interval between the two neighboring diffraction points are a constant, $\lambda F/d$, and are inversely proportional to the spatial period, d, of the grating. When the spatial frequency of the grating is f = 40 lines/mm and the wave-length of the project beam is λ = 514 nm, the minimum integral number $i = j \leq \pm\frac{1}{\lambda f} = \pm 48$

or i and $j \leq 0, \pm 1, \pm 2, \pm 3, \ldots, \pm 48$

Let an incidence coherent beam Illuminate the grating at an incident angle θ_1 as shown in Fig.2(b).

$$A(x)= A \cdot \exp[\frac{2\pi i}{\lambda} \sin(\theta_1 \cdot x)]$$

where $\exp[\frac{2\pi i}{\lambda} \sin\theta_1 \cdot x]$ denotes a linear phase factor and θ_1 delineates an arbitrary inclination angle of the beam in the z-x plane relative to the normal line, z. Let the spatial frequency of the grating $f_1 = \frac{\mathrm{Sin}\theta_1}{\lambda}$. On the Fourier's spectrum plane, the inclined Fraunhoffer diffraction field $U_{IA}[x',y']$ is

$$\begin{aligned} U_{IA}[x',y'] &= \mathcal{F}\ \{A \cdot [T(x,y)] \cdot \exp[2\pi\ i\ f_1 \cdot x]\} \\ &= A \cdot \mathcal{F}\ \{T(x,y)\} * \mathcal{F}\ \{\exp[2\pi i\ f_1 \cdot x]\} \\ &= A \cdot U_n[x', y'] * \delta(f_x - f_1) \\ &= \frac{A}{\lambda F} \cdot U_n[x', y'] * \delta\ (x' - F\sin\theta_1) \\ &= \frac{A}{\lambda F} \cdot U_n[\ (x' - F\sin\theta_1)\ , y'] \end{aligned}$$

Here the asterisk "*" is a symbol indicating that these functions are to be convoluted and "δ" represents a delta function. From this result we can see that the inclined Fraunhoffer diffraction field projection, $U_{IA}[x',y']$, has the same spectrum field as the normal projection, $U_n[x',y']$, except that x' is replaced by $(x'- F\sin\theta_1)$ which means that the whole diffraction field Un only moves a parallel distance, $-F\sin\theta_1$, toward the left side as shown in Fig. 2(b).

Similarly, a symmetric laser beam, B, with an incident angle, $-\theta_1$, has a Fraunhoffer diffraction spectrum field of

$$U_{IB}[x',y'] = \frac{B}{\lambda F} \cdot U_n\ [\ (x' + F\sin\theta_1\ )\ , y']$$

The whole diffraction field Un can then shift a distance $F\sin\theta_1$ toward the right side.

The two symmetric incident angles, θ_1 and $-\theta_1$, are then adjusted so that the condition $\sin\theta_1 = m \cdot \sin\theta = m\lambda f$ is satisfied, where "m" is the multiplication number. All points in the two diffraction fields will coincide, but will be of different diffraction order. Each pair of the arbitrary principal maximum points are formed by two coincident diffraction beams A(i+m,j)

and B(i-m,j), but all the coincident points have the same diffraction order differences of (2m,0) as shown in Fig.(2d). For example, when m = 1 the whole diffraction order differences are (2, 0) meaning that the multiplication numbers are 2 and 0 in the x and y direction, respectively. The condition of iso-optical path can be satisfied by any pair of the two groups of diffracted beams with the same diffraction angle shown in Fig. 3.

Let $U_{A(i+m,j)}(x,y)$ and $U_{B(i-m,j)}(x,y)$ represent the wave fronts of any pair of the two matched diffracted beams. Due to the iso-optical path, both beams, which are diffracted by the specimen grating at the same phase angle, will have a uniform zero phase difference, i.e. a null field. When the specimen grating is deformed due to specimen deformation, the two warping wave fronts are

$$U_{A(i+m,j)}(x,y) = A_{ij}\{\exp[i\Phi_A(x,y)]\}$$

$$U_{B(i-m,j)}(x,y) = B_{ij}\{\exp[i\Phi_B(x,y)]\}$$

where A_{ij} and B_{ij} are the amplitudes of the two diffracted beams in the direction of diffraction order (i,j). $\Phi_A(x,y)$ and $\Phi_B(x,y)$ represent the changes in the phase angles due to plane warping of the wave front.

Let p denote an arbitrary point in the specimen grating. As the specimen grating deforms, point p will move to a new location p' with u(x,y), v(x,y), and w(x,y) displacement as shown in Fig.4. The inclination angle of the two incident beams is $\sin\theta_1 = m\cdot\sin\theta$ and the changes in the corresponding phase angles are

$$\Phi_A(x,y) = \frac{2\pi}{\lambda}\{u(x,y)\sin\theta_1+(1+\cos\theta_1)w(x,y)]$$

$$\Phi_B(x,y) = \frac{2\pi}{\lambda}\{-u(x,y)\sin\theta_1+(1+\cos\theta_1)w(x,y)]$$

The intensity, I(x,y) can be expressed as a product of $[U_{A(i+m,j)}(x,y)+U_{B(i-m,j)}(x,y)]$ and its conjugation $[U_{A(i+m,j)}(x,y)+U_{B(i-m,j)}(x,y)]^*$

$$I(x,y)=[U_{A(i+m,j)}(x,y)+U_{B(i-m,j)}(x,y)][U_{A(i+m,j)}(x,y)+U_{B(i-m,j)}(x,y)]^*$$
$$= 4D^2\cos^2[\Phi_A(x,y) - \Phi_B(x,y)]$$
$$= 4D^2\cos^2 [\ \delta\ (x,y)/2]$$

When $A_{ij} = B_{ij} = 2D$, the phase difference, $\delta\ (x,y)$, between the two diffraction beams can be calculated as

$$\delta\ (x,y)= \Phi\ _A(x,y) - \Phi_B(x,y)$$
$$= \frac{2\pi m}{\lambda}\ [2u(x,y)]\ \mathrm{Sin}\theta$$
$$= 2\pi\, mf[2u(x,y)]$$

When $\delta(x,y) = 2k\pi$, the moire fringe pattern will be formed. Therefore

$$u(x,y) = \frac{k}{2mf}, \quad k = 0, \pm1, \pm2, \pm3,.....$$

The result indicates that the displacement field generated by the diffracted beams A_{ij} and $B_{i\,j}$ depend only on u(x,y) and are unaffected by the out-of-plane displacement w(x,y) which is generated by the lateral deformation of the specimen and the surface warping along the Z-axis. The total interference images will have the fringe pattern of the same order. Similarly one can prove that

$$v(x,y) = \frac{k}{2mf}, \quad k = 0, \pm1, \pm2, \pm3,.....$$

In the following, an experimental, which was included to verify the above theory, is described.

Experiment

The deep geometric grating consists of an ultra-thick semi-transparent film which is etched with a deep grating on a mirrored surface of the specimen. The film combines the function of a reference grating and a display screen. When the two coherent beam intersect on the specimen surface and the radiated diffraction beams are projected on to the screen of the film, the interference pattern can be observed clearly from any direction. For example, a grating of f=40 lines/mm in an argon laser field will project visible diffracted beams of about 9000 lines in different directions. The good contrast of the displacement patterns for large deformation or crack tip plastic zone is obtained even when the specimen surface is warped.

(1) Preparation of Steep Wall Profile Specimen Grating

Specimen gratings for a compact tension (CT) and an single edge notch (SEN) 2024-T3 specimens, as shown in Fig. 5, were fabricated following the procedure shown in Fig. 6. In order to enhance the diffraction efficiency of the grating, the specimen surface must be polished to a mirror grade . The steep grating and the display screen were made by spin coating a ultra-thick AZ4903 photo resist or by using the immersion method with a 1400 series photo resist. Either method will achieve a coating layer thickness of 5-10 μm which forms the grating after exposure and developing. Either photo resist can be exposed with a light source in the spectral range of 350-450 nm; i.e. a typical mercury exposure system. The energy for proper exposure requirement is approximately 30mJ/cm^2 per thickness μm. Usually glycerol is spread between the master grating and the coating layer to eliminate the ghost lines. After development, the photo resist has a convex and concave surface with frequency f. The specimen is then placed into a bath of 85% concentrate liquid phosphoric acid at a temperature of 70°C and etched to a steep wall profile.

(2) Compact u-v Set and Optical Path Arrangement

Since the grating spatial frequency of 40 lines/mm require an incidence angle between the z-axis and the two coherent beams of 1.176°, a special compact u-v set as shown in Fig. 7,

was designed. The optical path arrangement of the moire interferometry test is shown in Fig.8. The fringe patterns of typical u- and v-displacement fields corresponding to varying loads are displayed on the screen of the specimen surface are shown in Fig.9

Stable Crack Growth Studies

40 lines/mm steep geometric specimen gratings were produced on 2024-T3 compact tension (CT) and single edge notched (SEN) specimens, using the newly developed specimen grating transfer procedure [4]. Fracture tests were then conducted to evaluate the performance of the specimen grating under gradually increasing loads. Beyond the maximum load and with long crack extension, large plastic zone formed and specimen surface was warped but the Moiré fringes as shown in Figure 9, were clearly displayed on the surfaces of the specimen and could be viewed from any direction, The average number of v-displacement fringes over the length of a typical SEN specimen is $k_{ave} \approx 60$ lines in a 25 mm interval. Thus the elongation $\Delta\ell_{ave} = k_{ave} \times d \approx 60 \times 0.025 = 1.5$ mm, and the engineering strain in this interval can be expressed as;

$$\varepsilon_{ave} = \frac{\Delta\ell_{ave}}{\ell_0} = \frac{\Delta\ell_{ave}}{25\text{-}\Delta\ell_{ave}} \approx 0.063$$

In the plastic zone the average number of v-displacement fringes over the length is $k_{plastic} \approx 180$ lines per 25 mm, so that the plastic strain $\varepsilon_{plastic} \approx 0.189$.

Conclusion

The concept and theoretical background of a steep geometric grating for use in moiré interferometry are presented. The utility of a steep geometric grating is demonstrated in stable crack growth studies in 2024-T3 CT and SEN specimen.

Acknowledgements

This research was sponsored by the Office of Naval Research under ONR contract N00014-89-J-1276. The authors would like to thank Dr. Yapa D.S. Rajapakse for his support during the course of this investigation.

Reference

1. Joseph W. Goodman, "Introduction to Fourier Optics", McGraw-Hill Book Company, New York, (1968).
2. K. H. Zhou, and X. H. Zhong, " Optics,"Beijing University Press. (1984).
3. D. Post, "Optical Interference for Deformation Measurement - Classical Holographic and Moiré Interferometry," Mechanics of Nondestructive Testing. W.W. Stinchcomb, Ed., pp.1-53, Plenum. New York. (1980).
4. P.Ifju and D. Post, "Zero-Thickness Specimen Grating for Moiré Interferometry, "Experimental Techniques, 15(2), pp.45-47, March / April (1991).
5. F.X. Wang, B.S.-J. Kang and A.S. Kobayashi, "Composite Grating for Moiré Interferometry," Optical Engineering, Vol.29, No.7, pp.564-569, (July, 1988).
6 F.X. Wang and A.S. Kobayashi, "High Density Moiré Interferometry," Optical Engineering, Vol.29, No.1,pp.38-41, (Jan.,1990).
7. F.X. Wang, B.S.-J. Kang and K.Y. Lin, "Full-Field Displacements by Four-Beam Moiré Interferometry," Proceeding of the 1991 SEM Spring Conference, pp.278-284, Milwaukee, WI, (June, 1991).
8. G.B. May, F.X. Wang and A.S. Kobayashi, "Two-Parameter Crack Tip Field Associated with Stable Crack Growth -A Hybrid Analysis," Technical Report No. UWA/DME/TR-93-71.

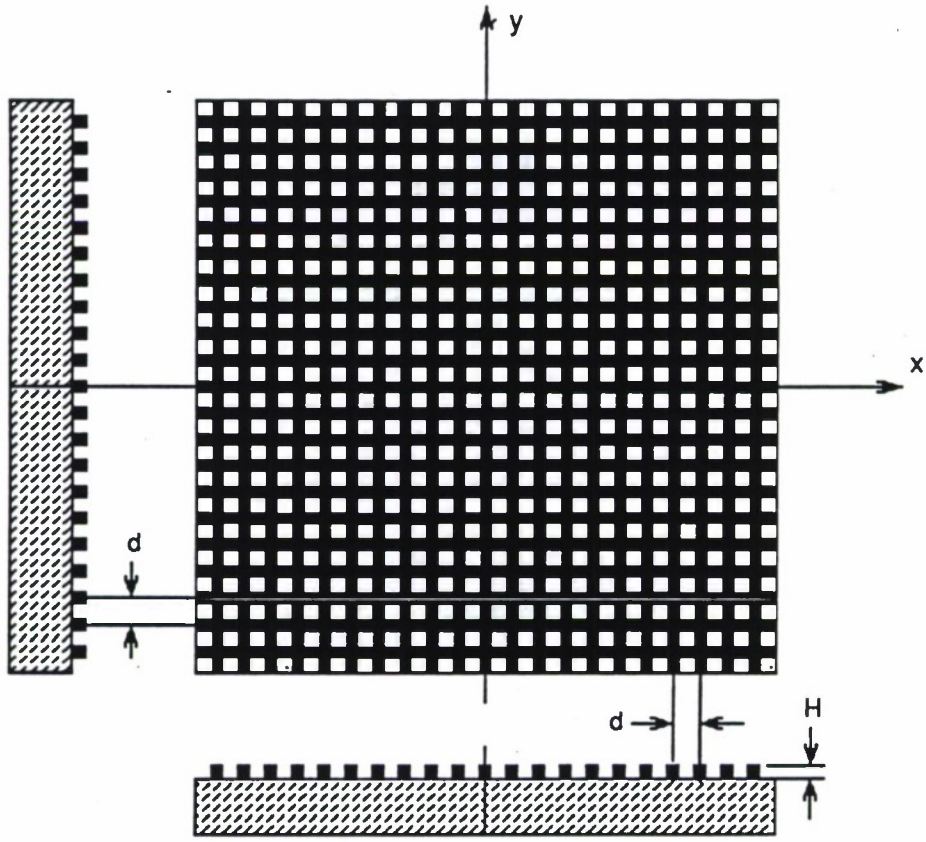

Fig. 1. The black and white grating

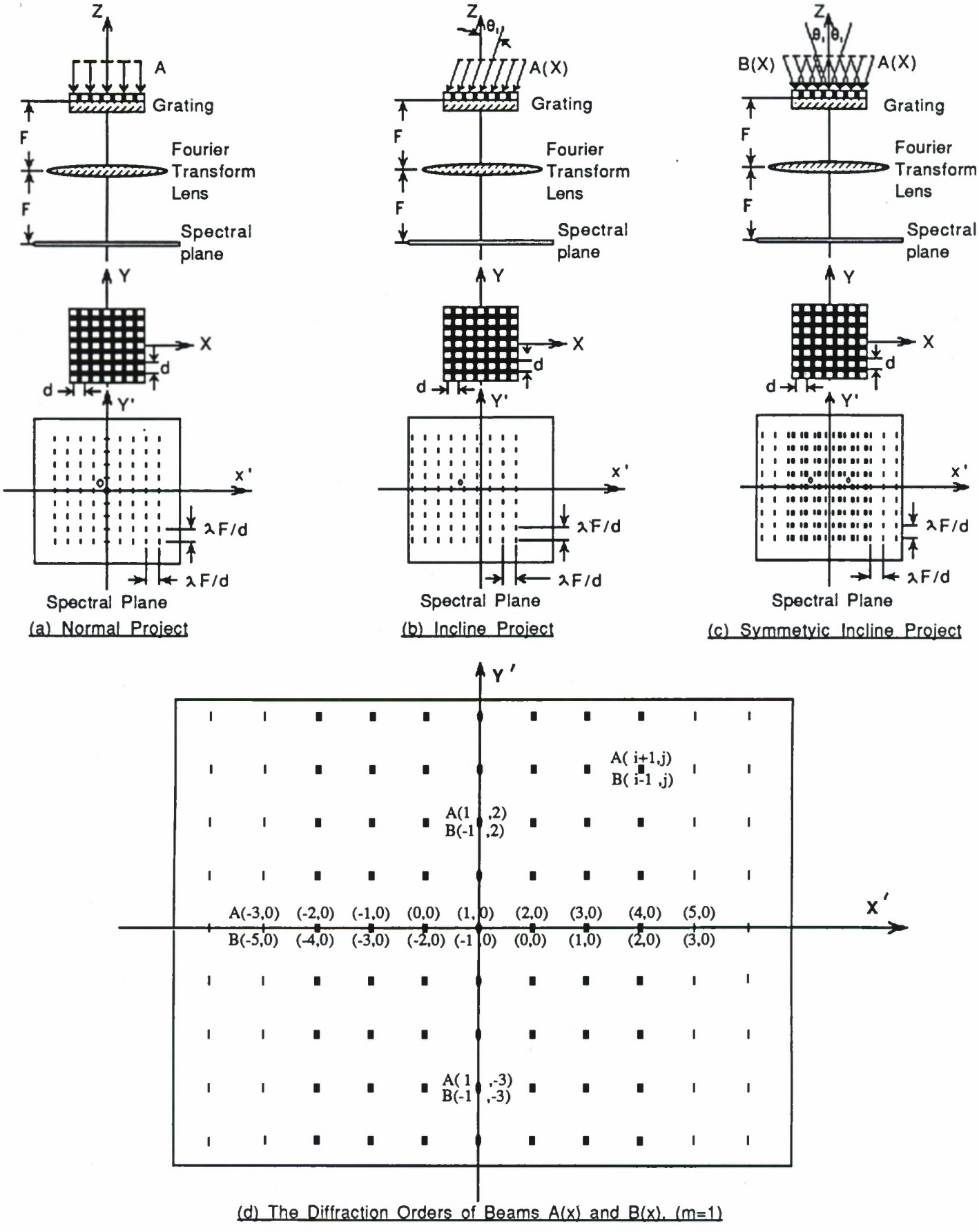

FIG. 2. Fraunhoffer diffraction field of black and white grating

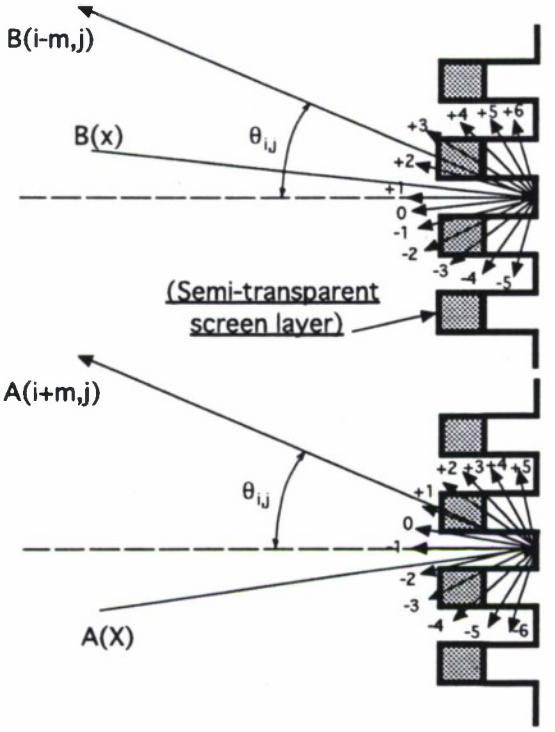

Fig. 3. Diffraction angle of steep grating

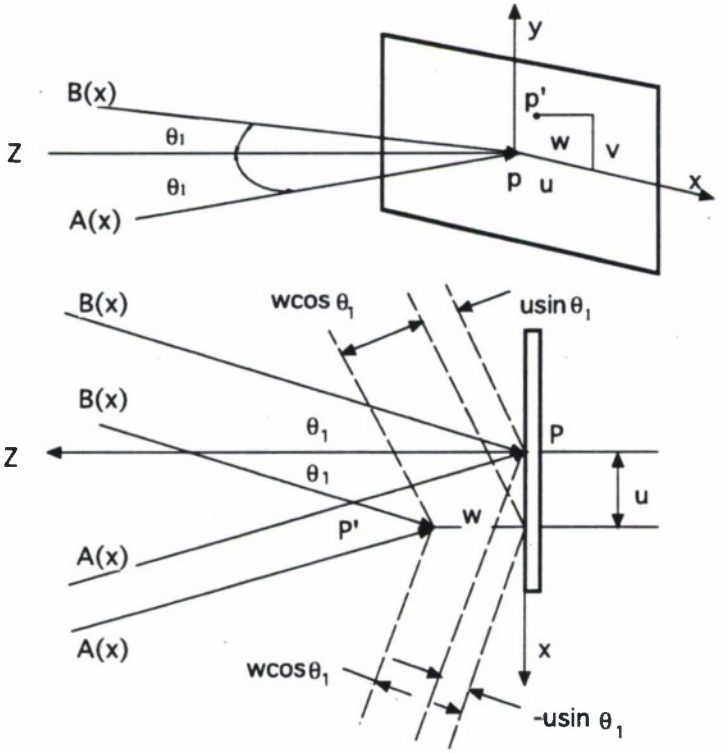

Fig. 4. u,v and w displacement and optical path difference

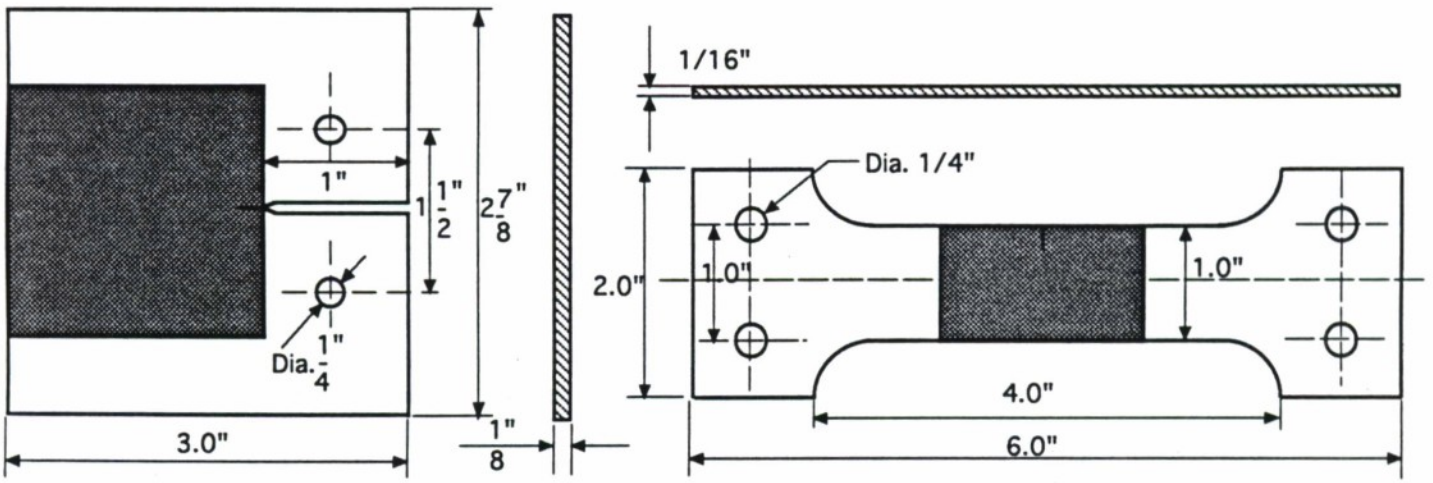

Compact tension specimen

Single edged notch specimen

Fig. 5. 2024 - T3 test specimen

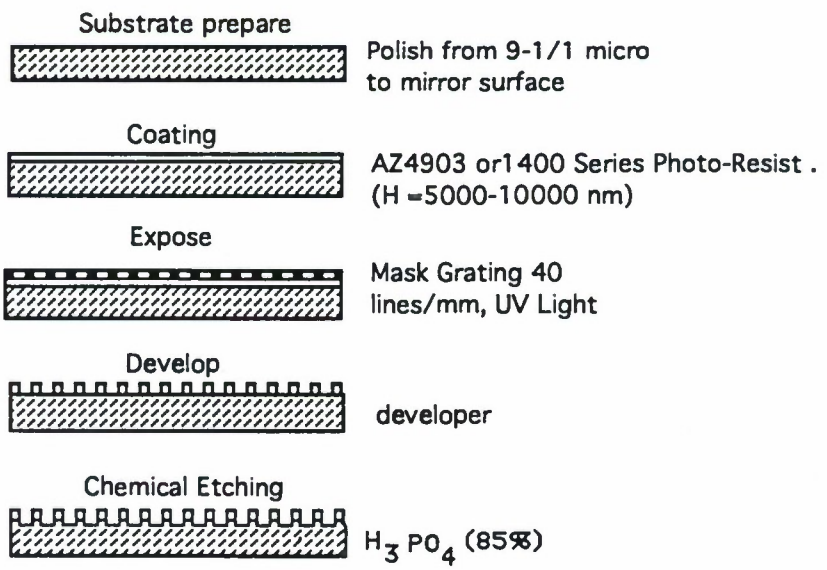

Fig. 6. The preparation of specimen grating

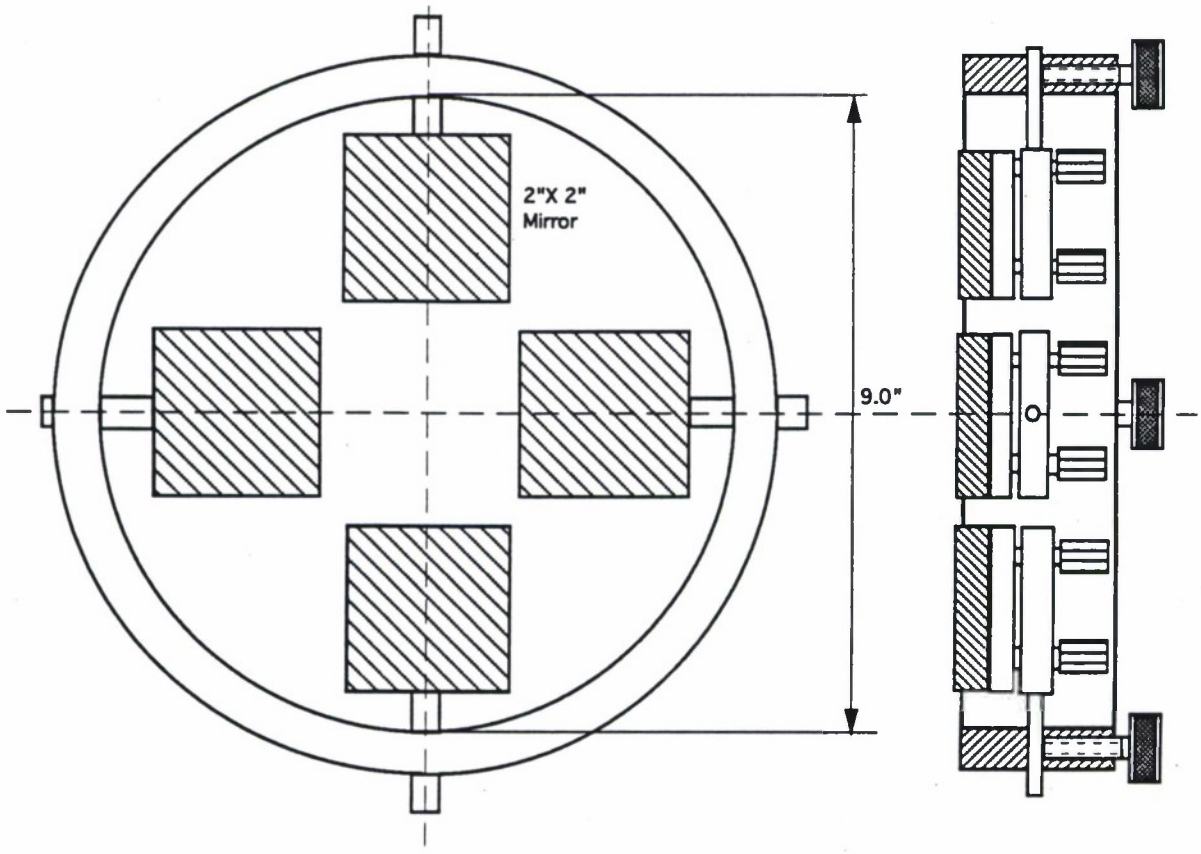

Fig. 7. Small u-v set (uesd for 40 lines/mm grating)

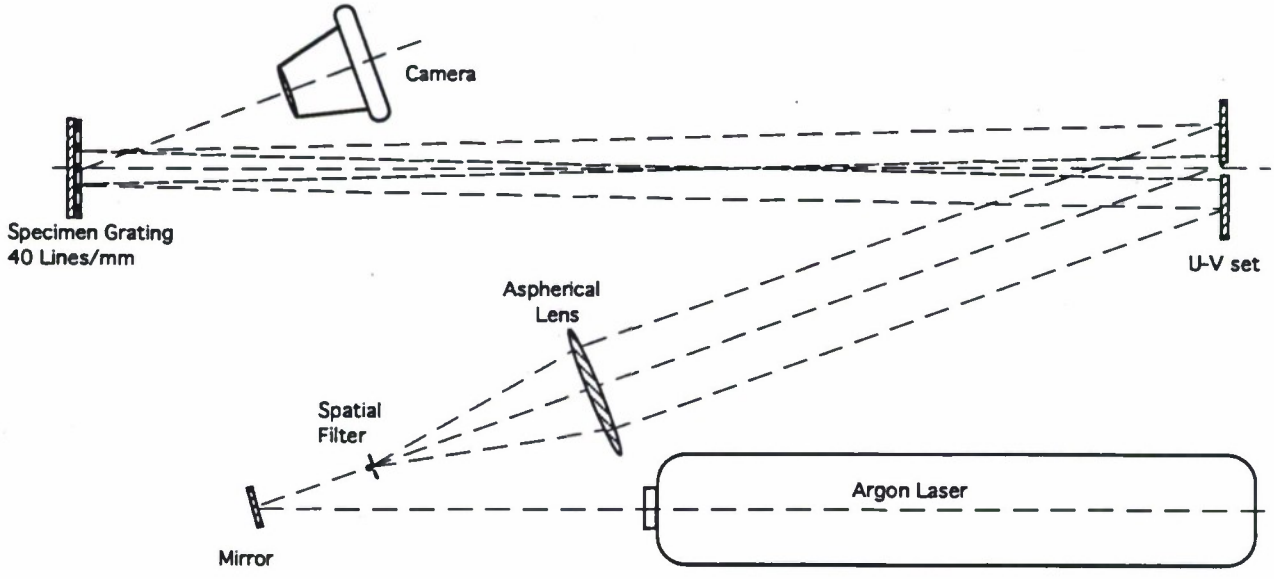

Fig.8. 40 lines/mm geometric grating used In moiré interferometry

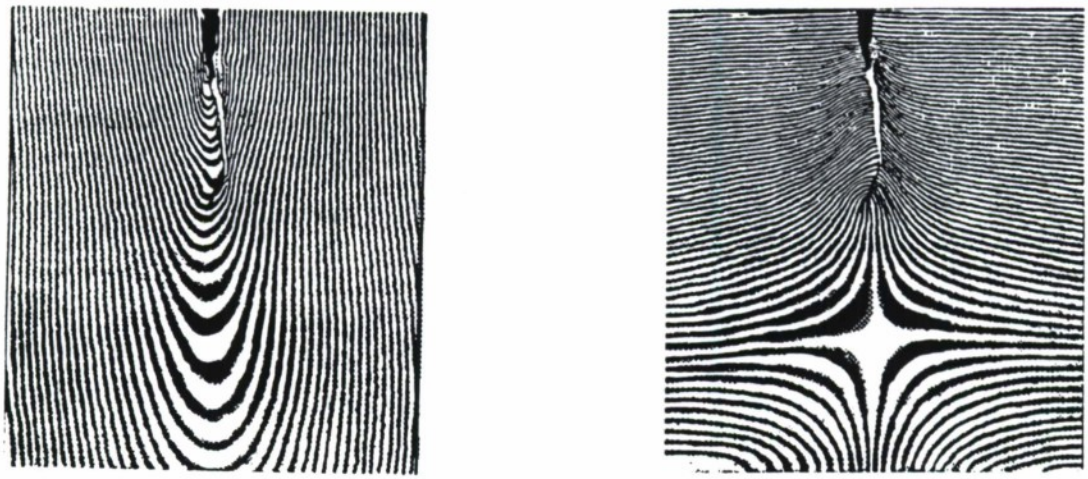

U-displacement V-displacement

CT-Specimen

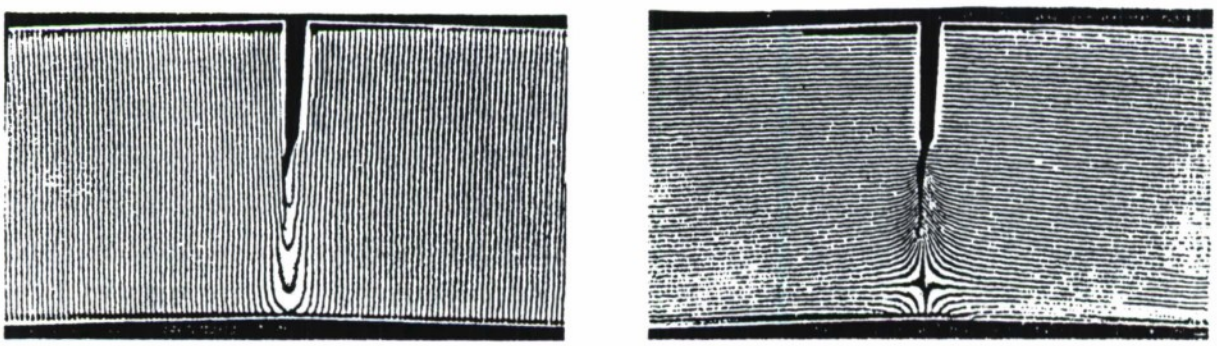

U-displacement V-displacement

SEN-Specimen

Fig. 9. Moire fringe pattern of CT and SEN specimens

REPORT DOCUMENTATION PAGE

Form Approved
OMB No. 0704-0188

1. AGENCY USE ONLY (Leave blank)	2. REPORT DATE	3. REPORT TYPE AND DATES COVERED
	July 1993	Technical Report

4. TITLE AND SUBTITLE
Steep Geometric Grating for Use in Moire Interferometry

5. FUNDING NUMBERS
N00014-J-1276

6. AUTHOR(S)
F.X. Wang, G.B. May and A.S. Kobayashi

7. PERFORMING ORGANIZATION NAME(S) AND ADDRESS(ES)
Department of Mechanical Engineering, FU-10
University of Washington
Seattle, WA 98195

8. PERFORMING ORGANIZATION REPORT NUMBER
UWA/DME/TR-93-73

9. SPONSORING/MONITORING AGENCY NAME(S) AND ADDRESS(ES)
Office of the Chief of Naval Research
Arlington, VA 22217-5000

10. SPONSORING/MONITORING AGENCY REPORT NUMBER

11. SUPPLEMENTARY NOTES

12a. DISTRIBUTION/AVAILABILITY STATEMENT
Unclassified

12b. DISTRIBUTION CODE
Unlimited

13. ABSTRACT (Maximum 200 words)

The theoretical background and the procedure of executing a new moire interferometry method, which combines the advantages of geometric moire method with the traditional moire interferometry, is reported. The method uses a steep geometric grating of about 40 lines/mm on a mirror finished specimen surface to achieve high contrast moire fringes. A special four beam moire interferometry bench is designed for the low grating frequency used. An application to experimental fracture mechanics analysis is briefly discussed.

14. SUBJECT TERMS
Geometric moire, moire interferometry, experimental stress analysis.

15. NUMBER OF PAGES
19

16. PRICE CODE

17. SECURITY CLASSIFICATION OF REPORT	18. SECURITY CLASSIFICATION OF THIS PAGE	19. SECURITY CLASSIFICATION OF ABSTRACT	20. LIMITATION OF ABSTRACT
Unclassified	Unclassified	Unclassified	None